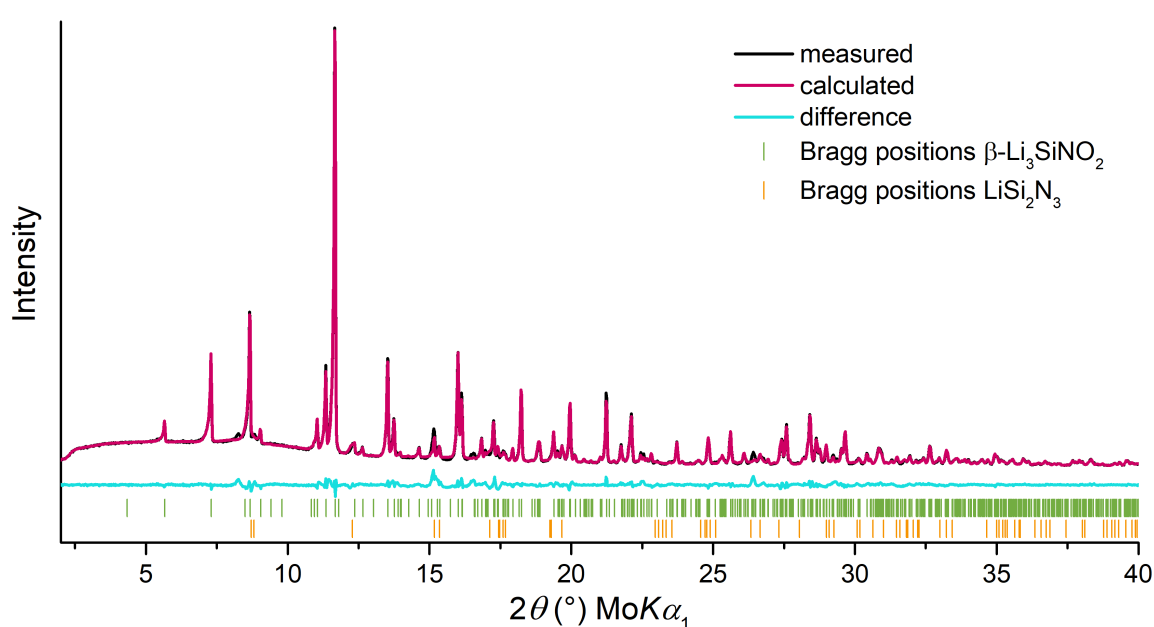


## Supplementary Information

### Polymorphism and polymorph-dependent luminescence properties of the first lithium oxonitridolithosilicate $\text{Li}_3\text{SiNO}_2:\text{Eu}^{2+}$

Kilian M. Rießbeck<sup>[a]</sup>, Daniel S. Wimmer<sup>[a]</sup>, Markus Seibald<sup>[b]</sup>, Dominik Baumann<sup>[b]</sup>, Klaus Wurst<sup>[a]</sup>, Gunter Heymann<sup>[a]</sup>, and Hubert Huppertz<sup>\*[a]</sup>

- [a] K. M. Rießbeck, D. S. Wimmer, Dr. K. Wurst,  
Assoc. Univ.-Prof. Dr. G. Heymann, Univ.-Prof. Dr. H. Huppertz:  
Department of General, Inorganic and Theoretical Chemistry,  
Universität Innsbruck  
Innrain 80-82, A-6020 Innsbruck, Austria  
E-Mail: [Hubert.Huppertz@uibk.ac.at](mailto:Hubert.Huppertz@uibk.ac.at)  
<https://www.uibk.ac.at/en/aatc/ag-huppertz>
- [b] Dr. M. Seibald, Dr. D. Baumann:  
ams-OSRAM International GmbH,  
Mittelstetter Weg 2, D-86830 Schwabmünchen, Germany



**Figure S1:** Rietveld refinement of the X-ray diffraction data from a powder sample of  $\beta\text{-Li}_3\text{SiNO}_2$ . The measured pattern is shown in black, the calculated pattern in red, the difference curve in turquoise and the tick marks of the

theoretical positions for the reflections are shown in green for  $\beta\text{-Li}_3\text{SiNO}_2$  and in orange for the side phase  $\text{LiSi}_2\text{N}_3$ .

**Table S1:** Report of the Rietveld refinements of the powder X-ray diffraction data from undoped and doped  $\beta\text{-Li}_3\text{SiNO}_2$  samples.

Parameter	Value (undoped sample)	Value (doped sample)
<b>Phase composition</b>		
$\beta\text{-Li}_3\text{SiNO}_2$ /wt%	95.1(2)	93.7(6)
$\text{LiSi}_2\text{N}_3$ /wt%	4.9(2)	6.3(6)
<b>Powder diffraction data of <math>\beta\text{-Li}_3\text{SiNO}_2</math></b>		
Diffractometer	STOE STADI P	
Radiation; wavelength / $\text{\AA}$	Mo-K $\alpha_1$ ; 0.7093	
$a$ / $\text{\AA}$	18.7462(5)	18.7451(7)
$b$ / $\text{\AA}$	11.1270(4)	11.1254(5)
$c$ / $\text{\AA}$	5.0897(2)	5.0916(2)
Cell volume / $\text{\AA}^3$	1061.66(5)	1061.83(7)
$2\theta$ range / $^\circ$	2 – 40	2 – 42
$2\theta$ step width / $^\circ$	0.015	0.015
$R_{\text{exp}}$ /%	1.78	5.31
$R_{\text{wp}}$ /%	6.14	8.40
$R_p$ /%	3.91	6.25
$R_{\text{Bragg}}$ /%	2.10	2.733

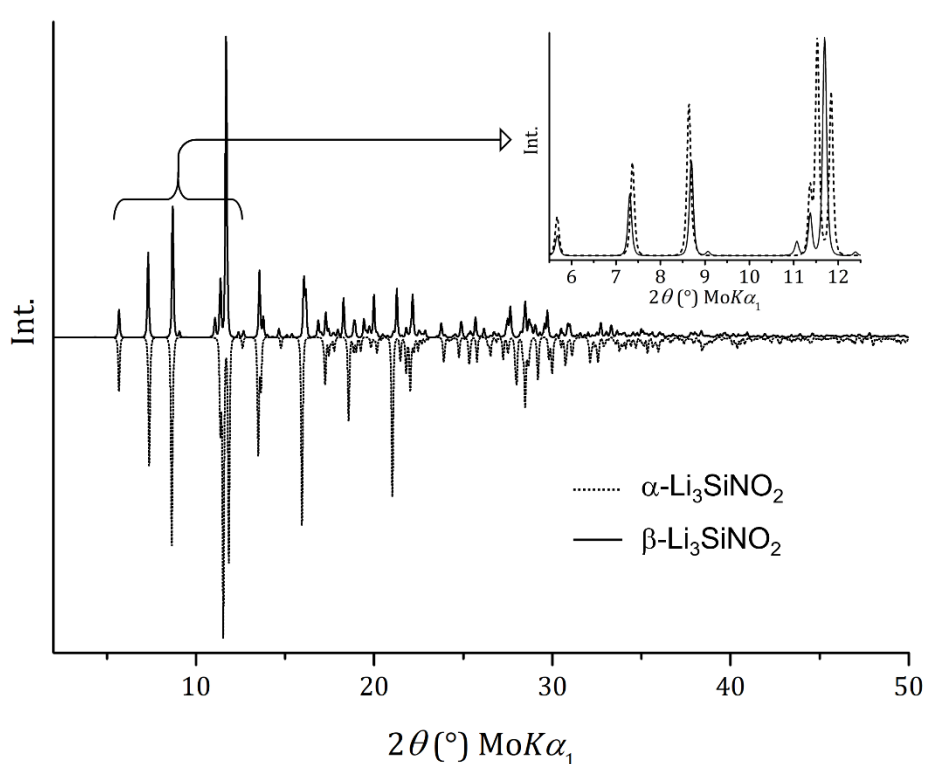


**Figure S2:** Comparison of the powder X-ray diffraction patterns for  $\alpha$ - (negative values/ dotted line) and  $\beta$ -Li<sub>3</sub>SiNO<sub>2</sub> (positive values/ solid line). The inset shows similarities and significant differences between the polymorphs in the lower diffraction angles.

**Table S2:** Wyckoff positions, atomic coordinates, and equivalent isotropic displacement parameters  $U_{\text{eq}}$  ( $\text{\AA}^2$ ) of orthorhombic  $\beta$ -Li<sub>3</sub>SiNO<sub>2</sub> (standard deviations in parentheses).

Atom	Wyckoff-Position	x	y	z	$U_{\text{eq}}$	occ.
Si1	8c	0.98497(2)	0.67981(5)	0.77906(9)	0.0141(2)	1
Si2	8c	0.76186(2)	0.67932(4)	0.17254(9)	0.0143(2)	1
O1	8c	0.93834(6)	0.5624(2)	0.6621(2)	0.0162(3)	1
O2	8c	0.80929(6)	0.5616(2)	0.2823(2)	0.0174(4)	1
O3	8c	0.92995(6)	0.3576(2)	0.2544(3)	0.0273(5)	1
O4	8c	0.67788(7)	0.6406(2)	0.2236(3)	0.0295(5)	1
N1	8c	0.96028(8)	0.6952(2)	0.1019(3)	0.0186(4)	1
N2	8c	0.78621(8)	0.6951(2)	0.8473(3)	0.0183(4)	1
Li1	8c	0.8728(2)	0.4583(2)	0.4744(4)	0.034(2)	0.9854(7)
Eu1	8c	0.8728(2)	0.4583(2)	0.4744(4)	0.000026(2)	0.0146(7)
Li2	8c	0.8783(2)	0.2303(3)	0.4774(5)	0.052(3)	0.9888(8)
Eu2	8c	0.8783(2)	0.2303(3)	0.4774(5)	0.000031(3)	0.0112(8)
Li3	8c	0.8737(2)	0.6836(3)	0.4728(7)	0.029(2)	1
Li4	8c	0.8716(2)	0.5747(5)	0.9658(9)	0.0279(9)	0.78
Li4a	8c	0.8733(8)	0.518(2)	0.964(3)	0.028(3)	0.22
Li5	8c	0.0144(2)	0.4493(3)	0.6988(7)	0.035(2)	1
Li6	8c	0.7488(2)	0.4395(3)	0.1271(7)	0.032(2)	1

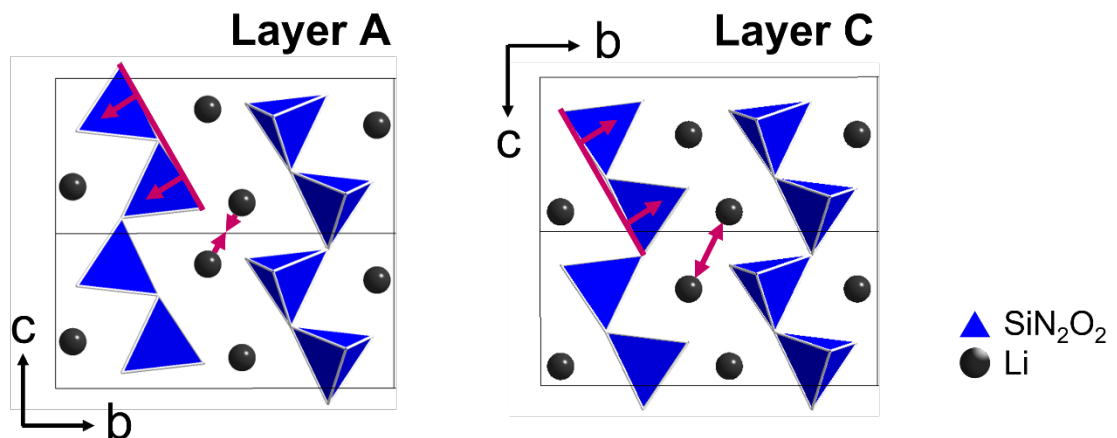
**Table S3:** Anisotropic displacement parameters  $U_{ij}$  ( $\text{\AA}^2$ ) of orthorhombic  $\beta$ -Li<sub>3</sub>SiNO<sub>2</sub> (standard deviations in parentheses).

Atom	$U_{11}$	$U_{22}$	$U_{33}$	$U_{12}$	$U_{13}$	$U_{23}$
Si1	0.0158(2)	0.0133(2)	0.0132(2)	-0.0002(2)	-0.0007(2)	-0.0008(2)
Si2	0.0164(2)	0.0129(2)	0.0135(2)	-0.0006(2)	0.0003(2)	-0.0001(2)
O1	0.0175(6)	0.0137(6)	0.0173(6)	0.0002(4)	0.0002(5)	-0.0017(4)
O2	0.0208(6)	0.0140(6)	0.0173(6)	-0.0017(5)	-0.0035(5)	0.0006(4)
O3	0.0181(7)	0.0300(9)	0.0337(8)	-0.0006(5)	0.0000(6)	-0.0100(6)
O4	0.0228(7)	0.0336(9)	0.0322(8)	-0.0046(6)	0.0044(6)	-0.0073(6)
N1	0.0280(7)	0.0138(7)	0.0139(7)	0.0001(6)	0.0006(6)	0.0011(5)
N2	0.0281(7)	0.0142(7)	0.0126(7)	0.0005(6)	-0.0020(6)	0.0001(5)
Li1	0.036(3)	0.038(3)	0.028(3)	0.003(2)	0.001(2)	0.003(2)

Li2	0.044(4)	0.062(6)	0.050(5)	-0.020(2)	-0.018(2)	0.018(2)
Li3	0.027(2)	0.016(2)	0.043(2)	0.000(2)	-0.018(2)	-0.001(2)
Li5	0.058(2)	0.029(2)	0.016(2)	0.027(2)	-0.001(2)	0.005(2)
Li6	0.048(2)	0.018(2)	0.026(2)	-0.014(2)	-0.014(2)	0.005(2)

**Table S4:** Interatomic distances of orthorhombic  $\beta$ -Li<sub>3</sub>SiNO<sub>2</sub> (standard deviations in parentheses).

Si1	- N1	1.716(2)			
	- N1	1.720(2)	$\emptyset$ Si1-N	1.718	
	- O1	1.680(2)			
	- O3	1.656(2)	$\emptyset$ Si1-O	1.668	
Si2	- N2	1.726(2)			
	- N2	1.718(2)	$\emptyset$ Si2-N	1.722	
	- O2	1.678(2)			
	- O4	1.652(2)	$\emptyset$ Si2-O	1.665	
Li1	- O1	1.941(3)			
	- O2	1.922(3)			
	- O3	1.912(3)			
	- O4	1.929(3)	$\emptyset$ Li1-O	1.926	
Li2	- O3	1.970(4)			
	- O3	2.056(4)			
	- O4	1.943(4)			
	- O4	2.178(4)	$\emptyset$ Li2-O	2.037	
Li3	- N1	2.210(4)			
	- N1	2.493(4)			
	- N2	2.216(4)			
	- N2	2.517(4)	$\emptyset$ Li3-N	2.359	
	- O1	2.053(4)			
	- O2	2.058(4)	$\emptyset$ Li3-O	2.056	
Li4	- N1	2.245(5)			
	- N2	2.172(5)	$\emptyset$ Li4-N	2.209	
	- O1	1.993(5)			
	- O2	1.995(5)			
	- O3	3.03(6)			
	- O4	2.85(6)	$\emptyset$ Li4-O	2.47	
Li4a	- N1	2.65(2)			
	- N2	2.63(2)	$\emptyset$ Li4a-N	2.64	
	- O1	2.02(2)			
	- O2	2.07(2)			
	- O3	2.55(2)			
	- O4	2.35(2)	$\emptyset$ Li4a-O	2.25	
Li5	- N1	1.960(4)			
	- O1	1.910(4)			



	- O1	2.043(4)		
	- O3	2.400(4)		
			$\emptyset \text{ Li5-O}$	2.118
<hr/>	<hr/>	<hr/>	<hr/>	<hr/>
Li6	- N2	1.983(4)		
	- O2	1.938(4)		
	- O2	2.065(4)		
	- O4	2.627(4)		
	- O4	2.649(4)	$\emptyset \text{ Li6-O}$	2.320

**Figure S3:** Comparison of excerpts of layer A (left) and C (right) of  $\beta\text{-Li}_3\text{SiNO}_2$  with the differences relevant to the changed connection scheme marked in red. For clarity, the anions are not shown here.

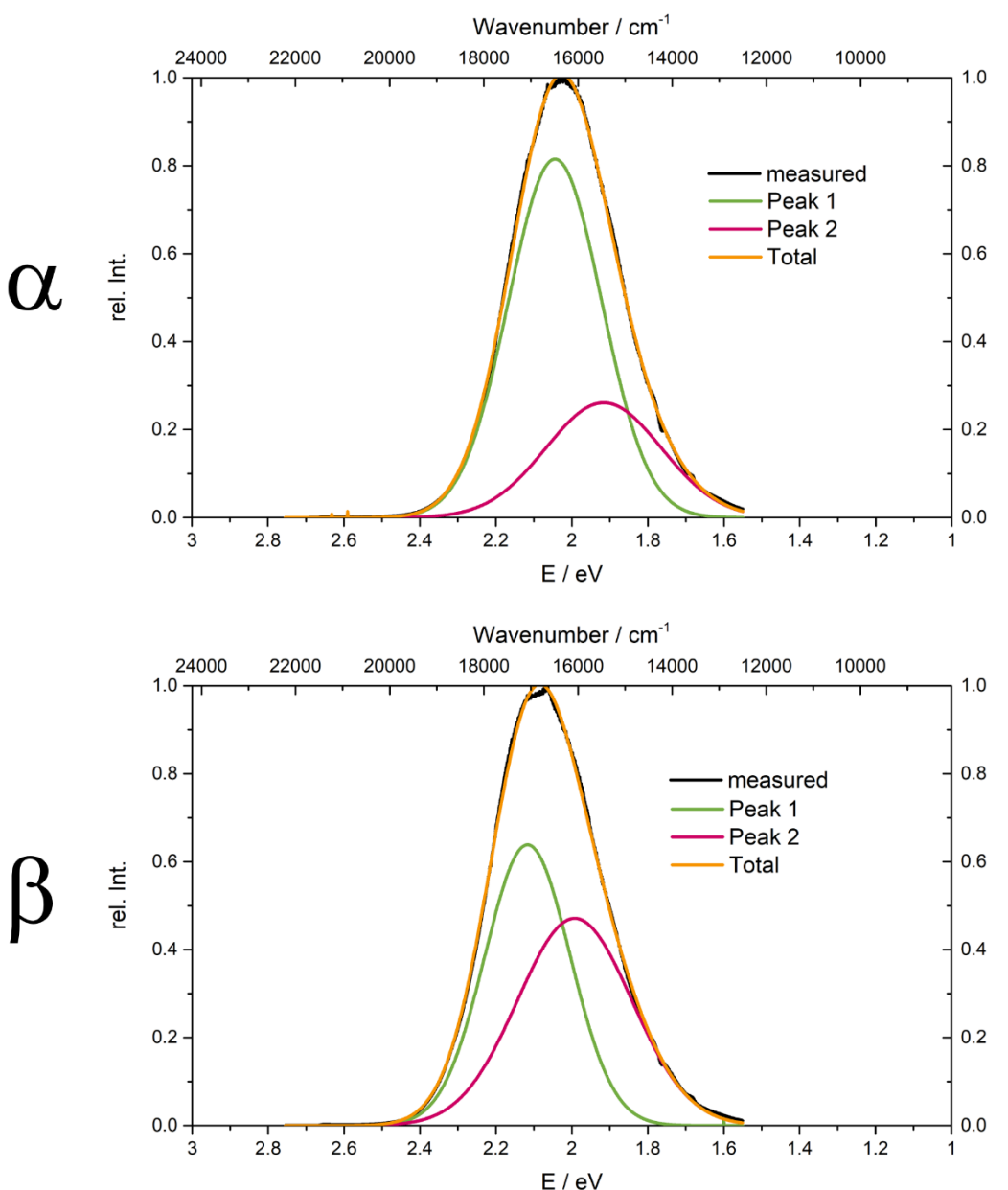


**Figure S4:** Bimodal Gauß-fits of the emission spectra obtained from powder samples of  $\alpha$ - and  $\beta$ - $\text{Li}_3\text{SiNO}_2:\text{Eu}^{2+}$ .

**Table S5:** Parameters of the two Gauß-curves of the decomposition of the emission spectra from powder samples of  $\alpha$ - and  $\beta$ - $\text{Li}_3\text{SiNO}_2:\text{Eu}^{2+}$ .

	$\alpha\text{-Li}_3\text{SiNO}_2$		$\beta\text{-Li}_3\text{SiNO}_2$	
	Peak 1	Peak 2	Peak 1	Peak 2
rel. Intensity	0.72	0.28	0.50	0.50
$E_{\text{peak}} / \text{eV}$	2.04	1.92	2.12	1.99
$\tilde{\nu}_{\text{peak}} / \text{cm}^{-1}$	16488	15456	17072	16071
FWHM / eV	0.29	0.36	0.26	0.35
FWHM / $\text{cm}^{-1}$	2323	2886	2130	2850

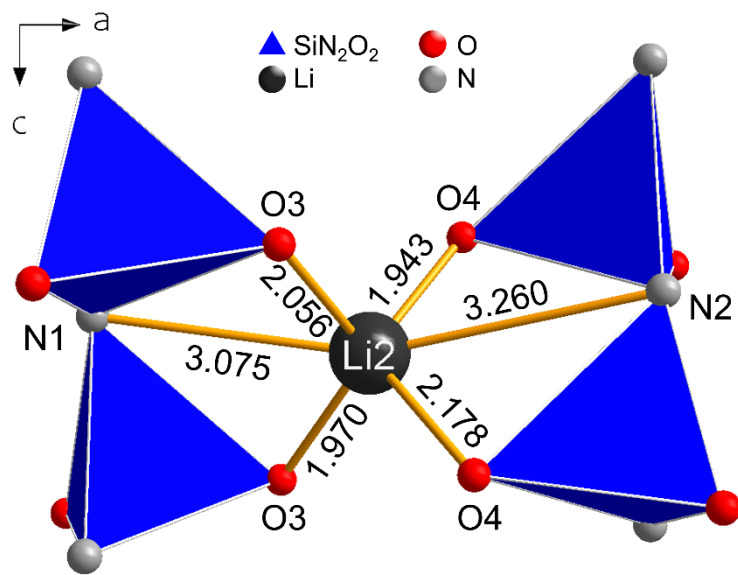


**Figure S5:** The local environment of the  $\text{Li}_2$ -position in  $\beta\text{-Li}_3\text{SiNO}_2:\text{Eu}^{2+}$  is shown with its bond lengths in a 4+2 coordination.